Proportional–integral-plus (PIP) control of the ALSTOM gasifier problem

C J Taylor, A P McCabe, P C Young and **A Chotai***
Centre for Research on Environmental Systems and Statistics, Lancaster University, UK

Abstract: Although it is able to exploit the full power of optimal state variable feedback within a non-minimum state-space (NMSS) setting, the proportional–integral-plus (PIP) controller is simple to implement and provides a logical extension of conventional proportional–integral and proportional–integral–derivative (PI/PID) controllers, with additional dynamic feedback and input compensators introduced automatically by the NMSS formulation of the problem when the process is of greater than first order or has appreciable pure time delays. The present paper applies the PIP methodology to the ALSTOM benchmark challenge, which takes the form of a highly coupled multivariable linear model, representing the gasifier system of an integrated gasification combined cycle (IGCC) power plant. In particular, a straightforwardly tuned discrete-time PIP control system based on a reduced-order backward-shift model of the gasifier is found to yield good control of the benchmark, meeting most of the specified performance requirements at three different operating points.

Keywords: proportional–integral-plus (PIP), linear quadratic (LQ), multi-objective optimization, multi-variable control design, ALSTOM gasifier benchmark

NOTATION

$\mathbf{D}$	state-space command input matrix
$\mathbf{F}$	state-space transition matrix
$\mathbf{G}$	state-space input matrix
$\mathbf{H}$	state-space observation matrix
$\mathbf{K}$	control gain matrix
m	order of the matrix fraction description numerator
n	order of the matrix fraction description denominator
$\mathbf{Q}$	linear quadratic state weighting matrix
$\mathbf{R}$	linear quadratic input weighting matrix
$u_1^{\mathrm{w}}, \ldots, u_p^{\mathrm{w}}$	input weighting parameters
$\boldsymbol{u}(k)$	input vector
$\boldsymbol{x}(k)$	state vector
$y_1^{\mathrm{w}}, \ldots, y_p^{\mathrm{w}}$	output weighting parameters
$\boldsymbol{y}(k)$	output vector
$\boldsymbol{y}_{\mathrm{d}}(k)$	vector of command (desired) inputs
z^{-i}	backward-shift operator, $z^{-i}y(k) = y(k-i)$
$z_1^{\mathrm{w}}, \ldots, z_p^{\mathrm{w}}$	integral-of-error weighting parameters
$\boldsymbol{z}(k)$	vector of integral-of-error states

The MS was received on 17 July 2000 and was accepted after revision for publication on 11 September 2000.
** Corresponding author: Centre for Research on Environmental Systems and Statistics, Lancaster University, Lancaster LA1 4YQ, UK.*

1 INTRODUCTION

Previous papers have introduced the proportional–integral-plus (PIP) controller [**1–3**], in which non-minimal state-space (NMSS) models are formulated so that full-state variable feedback control can be implemented directly from the measured input and output signals of the controlled process, without resort to the design and implementation of a deterministic state reconstructor (observer) or a stochastic Kalman filter. Over the last few years, PIP control systems have been successfully employed in a range of practical applications (see, for example, references [**4**] to [**6**]).

The PIP controller can be interpreted as a logical extension of conventional proportional–integral (PI) and proportional–integral–derivative (PID) controllers, with additional dynamic feedback and input compensators introduced automatically by the NMSS formulation of the problem when the process has second-order or higher dynamics or pure time delays greater than one sampling interval [**7**]. In contrast with conventional PI and PID controllers, however, the PIP design has numerous advantages; in particular, its structure exploits the power of state variable feedback (SVF) methods, where the vagaries of manual tuning are replaced by pole assignment or linear quadratic (LQ) design. With regard to the latter of these, it is worth noting that, due to the special structure of the non-minimal state vector, the

elements of the LQ weighting matrices have a particularly simple interpretation, since the diagonal elements directly define weights assigned to the measured variables.

Integrated gasification combined cycle (IGCC) power plants aim to provide environmentally clean and efficient power generation from coal. ALSTOM have developed and validated a non-linear dynamic simulation model of a pilot integrated plant based upon the air-blown gasification cycle [**8**]. The model includes all the significant components of the system, including the drying of coal and limestone, the pyrolysis and volatilization of coal, and the gasification process itself. The subject of the benchmark challenge, however, is a linear 25th-order continuous-time state-space system, derived from the non-linear model at three different operating points, representing the gasifier at 100, 50 and 0 per cent load.

The model includes five actuators, all flowrates with units of kilograms per second: WCHR (char extraction); WAIR (air mass); WCOL (coal mass); WSTM (steam mass); WLS (limestone mass). However, the specifications require that, since limestone absorbs sulphur in the coal, WLS is always set to 10 per cent of the value of WCOL, effectively leaving four controllable inputs to decouple the four outputs. These outputs include CVGAS [fuel calorific value (kJ/kg)], MASS [bed mass (kg)], PGAS [fuel gas pressure (kN/m^2)] and TGAS [fuel gas temperature (K)]. Finally, the model incorporates a disturbance signal PSINK [sink pressure (kN/m^2)] representing the pressure upstream of the gas turbine, which in practice varies according to the position of the gas turbine fuel valve. The benchmark challenge involves carrying out specific performance tests using a controller optimized for the 100 per cent load operating point. To investigate the robustness of the designs, the controller is also evaluated on the models representing the gasifier at 50 and 0 per cent load. The full specifications of the plant, together with the control objectives and performance tests, have been described by the ALSTOM contribution to the present issue [**8**].

2 NMSS–PIP DESIGN

Multi-variable PIP control can be applied to systems represented by discrete-time backward shift [**4**] and delta (δ) operator [**9**] or continuous-time (derivative operator) models [**10**]. However, backward-shift methods are employed for the research described below since they are so straightforward and yet are found to yield very good control of the 'stiff' gasifier system, which includes an array of fast and very slow dynamic modes. In this case, consider the following p-input p-output discrete-time system represented in terms of the left matrix fraction description:

$$\boldsymbol{y}(k) = [\mathbf{A}(z^{-1})]^{-1}\mathbf{B}(z^{-1})\boldsymbol{u}(k) \tag{1}$$

where

$$\boldsymbol{y}(k) = [y_1(k) \quad y_2(k) \quad \cdots \quad y_p(k)]^{\mathrm{T}}$$

$$\boldsymbol{u}(k) = [u_1(k) \quad u_2(k) \quad \cdots \quad u_p(k)]^{\mathrm{T}}$$

$$\mathbf{A}(z^{-1}) = \mathbf{I} + \mathbf{A}_1 z^{-1} + \cdots + \mathbf{A}_n z^{-n}$$

$$\mathbf{B}(z^{-1}) = \mathbf{B}_1 z^{-1} + \cdots + \mathbf{B}_m z^{-m}$$

Here, $\boldsymbol{y}(k)$ and $\boldsymbol{u}(k)$ are vectors of the system outputs and control inputs respectively, $\mathbf{A}_i$ $(i = 1, 2, \ldots, n)$ and $\mathbf{B}_i$ $(i = 1, 2, \ldots, m)$ are p by p matrices, while z^{-i} is the backward-shift operator, i.e. $z^{-i}y(k) = y(k-i)$. Note that some of the initial $\mathbf{B}_i$ terms can take null values to accommodate pure time delays in the system.

The model in equation (1) is formulated from the transfer functions identified for each input–output pathway of the multi-variable system. In the NMSS–PIP approach to control design, these transfer functions are usually identified from measured input–output data, collected either from planned experiments or during the normal operation of the plant. Alternatively, as in the present gasifier example, they are obtained from a data-based model reduction exercise (see, for example, reference [**11**]) conducted on a high-order simulation model of the system (here, this is a high-order linear model, but the same approach could be used with the non-linear model, where it performs combined linearization and reduction). In all cases, however, it is recommended that the required identification and estimation analysis should utilize the simplified refined instrumental variable (SRIV) algorithm [**12**, **13**] since it is often more effective in this regard than alternatives, such as the methods available in the MATLAB identification toolbox.

2.1 Non-minimal state-space form

The state vector for the NMSS form of equation (1) is defined as

$$\boldsymbol{x}(k)^{\mathrm{T}} = [\boldsymbol{y}(k)^{\mathrm{T}} \quad \boldsymbol{y}(k-1)^{\mathrm{T}} \quad \cdots \quad \boldsymbol{y}(k-n+1)^{\mathrm{T}} \quad \boldsymbol{u}(k-1)^{\mathrm{T}} \quad \cdots \quad \boldsymbol{u}(k-m+1)^{\mathrm{T}} \quad \boldsymbol{z}(k)^{\mathrm{T}}] \tag{2}$$

where $\boldsymbol{z}(k)$ is the following integral-of-error vector:

$$\boldsymbol{z}(k) = \boldsymbol{z}(k-1) + [\boldsymbol{y}_{\mathrm{d}}(k) - \boldsymbol{y}(k)] \tag{3}$$

in which $\boldsymbol{y}_{\mathrm{d}}(k)$ is the reference or command input vector, each element being associated with the relevant system output. Having defined the above state vector, the NMSS representation can be formulated directly in the following form:

$$\boldsymbol{x}(k) = \mathbf{F}\boldsymbol{x}(k-1) + \mathbf{G}\boldsymbol{u}(k-1) + \mathbf{D}\boldsymbol{y}_{\mathrm{d}}(k)$$

$$\boldsymbol{y}(k) = \mathbf{H}\boldsymbol{x}(k) \tag{4}$$

where the state matrices are defined as follows:

$$\mathbf{F}=\begin{bmatrix} -\mathbf{A}_1 & -\mathbf{A}_2 & \cdots & -\mathbf{A}_{n-1} & -\mathbf{A}_n & \mathbf{B}_2 & \cdots & \mathbf{B}_{m-1} & \mathbf{B}_m & \mathbf{0} \\ \mathbf{I}_p & \mathbf{0} & \cdots & \mathbf{0} & \mathbf{0} & \mathbf{0} & \cdots & \mathbf{0} & \mathbf{0} & \mathbf{0} \\ \mathbf{0} & \mathbf{I}_p & \cdots & \mathbf{0} & \mathbf{0} & \mathbf{0} & \cdots & \mathbf{0} & \mathbf{0} & \mathbf{0} \\ \vdots & \vdots & \ddots & \vdots & \vdots & \vdots & \ddots & \vdots & \vdots & \vdots \\ \mathbf{0} & \mathbf{0} & \cdots & \mathbf{I}_p & \mathbf{0} & \mathbf{0} & \cdots & \mathbf{0} & \mathbf{0} & \mathbf{0} \\ \mathbf{0} & \mathbf{0} & \cdots & \mathbf{0} & \mathbf{0} & \mathbf{0} & \cdots & \mathbf{0} & \mathbf{0} & \mathbf{0} \\ \mathbf{0} & \mathbf{0} & \cdots & \mathbf{0} & \mathbf{0} & \mathbf{I}_r & \cdots & \mathbf{0} & \mathbf{0} & \mathbf{0} \\ \vdots & \vdots & \ddots & \vdots & \vdots & \vdots & \ddots & \vdots & \vdots & \vdots \\ \mathbf{0} & \mathbf{0} & \cdots & \mathbf{0} & \mathbf{0} & \mathbf{0} & \cdots & \mathbf{I}_r & \mathbf{0} & \mathbf{0} \\ \mathbf{A}_1 & \mathbf{A}_2 & \cdots & \mathbf{A}_{n-1} & \mathbf{A}_n & -\mathbf{B}_2 & \cdots & -\mathbf{B}_{m-1} & -\mathbf{B}_m & \mathbf{I}_p \end{bmatrix}, \quad \mathbf{G}=\begin{bmatrix} \mathbf{B}_1 \\ \mathbf{0} \\ \mathbf{0} \\ \vdots \\ \mathbf{0} \\ \mathbf{I}_r \\ \mathbf{0} \\ \vdots \\ \mathbf{0} \\ -\mathbf{B}_1 \end{bmatrix}, \quad \mathbf{D}=\begin{bmatrix} \mathbf{0} \\ \mathbf{0} \\ \mathbf{0} \\ \vdots \\ \mathbf{0} \\ \mathbf{0} \\ \mathbf{0} \\ \vdots \\ \mathbf{0} \\ \mathbf{I}_p \end{bmatrix}$$

and $\mathbf{H}=\lfloor \mathbf{I}_p \ \mathbf{0} \ \cdots \ \mathbf{0} \rfloor$. Inherent type 1 servomechanism performance is introduced by means of the integral-of-error part of the state vector, $\boldsymbol{z}(k)$. If the closed-loop system is stable, then this ensures that steady state decoupling is inherent in the basic design [**4**].

2.2 Proportional–integral-plus control

The SVF control law associated with the NMSS model (4) is defined in the usual fashion:

$$\boldsymbol{u}(k)=-\mathbf{K}\boldsymbol{x}(k) \tag{5}$$

where $\mathbf{K}$ is the control gain matrix. This strategy results in a control system which can be structurally related to more conventional designs, such as multi-variable PI and PID controllers, as illustrated in Fig. 1a. Here,

$$\begin{aligned} \mathbf{L}(z^{-1})&=\mathbf{L}_0+\mathbf{L}_1 z^{-1}+\cdots+\mathbf{L}_{n-1}z^{-n+1} \\ \mathbf{M}(z^{-1})&=\mathbf{M}_1 z^{-1}+\cdots+\mathbf{M}_{m-1}z^{-m+1} \\ \mathbf{I}&=\mathbf{k_I}(1-z^{-1})^{-1} \end{aligned} \tag{6}$$

Incorporating the control law (5), the equation for the closed-loop system becomes

$$\boldsymbol{x}(k)=(\mathbf{F}-\mathbf{GK})\boldsymbol{x}(k-1)+\mathbf{D}\boldsymbol{y}_{\mathrm{d}}(k) \tag{7}$$

and, since full NMSS feedback is being used, the poles (or eigenvalues) of $(\mathbf{F}-\mathbf{GK})$ can be arbitrarily assigned if and only if the pair $[\mathbf{F},\mathbf{G}]$ is completely controllable. It is well known, however, that assignment of the closed-loop poles of a multi-variable system does not, in itself, uniquely specify the feedback gain matrix $\mathbf{K}$. Consequently a number of algorithms have been proposed for obviating this problem, e.g. the use of dyadic feedback or the Luenberger canonical form. The unrestrictive controllability conditions and the Luenberger canonical form for the NMSS model have been described by Chotai *et al.* [**14**].

Alternatively, as here, the SVF nature of the design method ensures that it can be used as a foundation for the design of PIP LQ controllers. Here, in the simplest infinite-time case, the requirement is to design a control gain matrix which minimizes the following quadratic

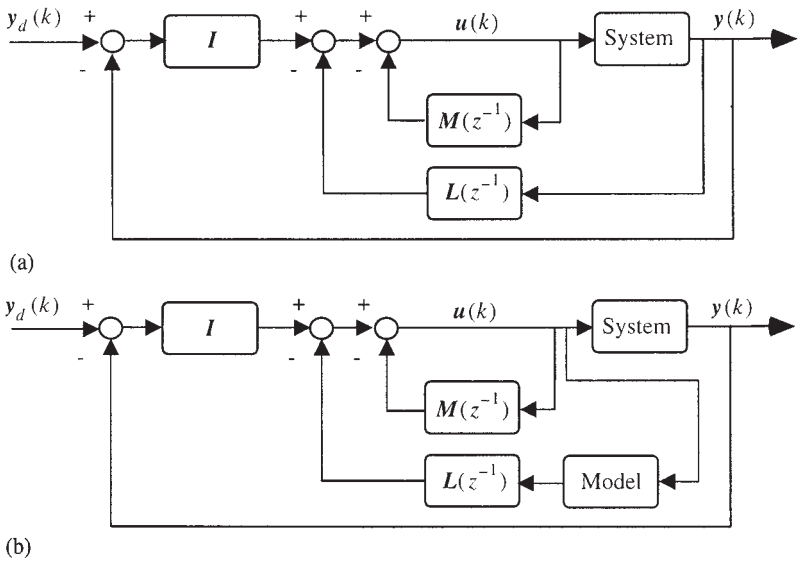

Fig. 1 Multi-variable PIP control (a) in feedback form and (b) in forward path form

performance criterion:

$$J = \sum_{i=0}^{\infty} \boldsymbol{x}(i)^{\mathrm{T}}\mathbf{Q}\boldsymbol{x}(i) + \boldsymbol{u}(i)^{\mathrm{T}}\mathbf{R}\boldsymbol{u}(i) \tag{8}$$

where $\mathbf{Q}$ and $\mathbf{R}$ are symmetric positive semidefinite and symmetric positive definite weighting matrices respectively. The feedback gain matrix which minimizes the cost function can be determined by the steady state solution of the discrete-time matrix Riccati equation (see, for example, reference [**15**]; note that this method does not require a non-singular $\mathbf{F}$ matrix). Here, to ensure a unique solution and closed-loop stability, the pair $[\mathbf{F}, \mathbf{Q}^{1/2}]$ should have no observable modes on the unit circle.

It is clear that, due to the special structure of the non-minimal state vector, the elements of the LQ weighting matrices have a particularly simple interpretation, since the diagonal elements directly define the weights assigned to the measured input and output variables, together with the integral-of-error states. In this regard, the following convention is employed for the choice of the multi-variable weighting matrices $\mathbf{Q}$ and $\mathbf{R}$:

$$\mathbf{Q} = \mathrm{diag}[\bar{y}_1 \quad \cdots \quad \bar{y}_n \quad \bar{u}_1 \quad \cdots \quad \bar{u}_{m-1} \quad \bar{z}] \tag{9}$$

where $\bar{y}_i$ $(i = 1, \ldots, n)$, $\bar{u}_i$ $(i = 1, \ldots, m-1)$ and $\bar{z}$ are all vectors of length p, with elements defined as follows:

$$\begin{aligned}
\bar{y}_i\,(i = 1, \ldots, n) &= \left[\frac{y_1^{\mathrm{w}}}{n} \cdots \frac{y_p^{\mathrm{w}}}{n}\right] \\
\bar{u}_i\,(i = 1, \ldots, m-1) &= \left[\frac{u_1^{\mathrm{w}}}{m} \cdots \frac{u_p^{\mathrm{w}}}{m}\right] \\
\bar{z} &= [z_1^{\mathrm{w}} \cdots z_p^{\mathrm{w}}]
\end{aligned} \tag{10}$$

in which, finally, $y_1^{\mathrm{w}}, \ldots, y_p^{\mathrm{w}}$, $u_1^{\mathrm{w}}, \ldots, u_p^{\mathrm{w}}$ and $z_1^{\mathrm{w}}, \ldots, z_p^{\mathrm{w}}$ are the user-selected weighting parameters. The corresponding input weighting matrix takes the following form:

$$\mathbf{R} = \mathrm{diag}\left[\frac{u_1^{\mathrm{w}}}{m} \cdots \frac{u_p^{\mathrm{w}}}{m}\right] \tag{11}$$

Although convoluted in description, the purpose of equations (9) to (11) is to simplify the choice of the LQ weightings, so that the designer selects only a *total* weight for (all the present and past values of) each input and output signal together with each integral of error state. Such a formulation is particularly useful when tuning the controller to meet the objectives of the present benchmark problem. The 'default' weightings are obtained by setting each of the user selected parameters to unity.

In the present research, adequate closed-loop control responses were quickly obtained by manually tuning these parameters. However, one recently developed technique available for *automatically* mapping the various control requirements into elements of the $\mathbf{Q}$ and $\mathbf{R}$ matrices (including the off-diagonal elements), is multi-objective optimization in its goal attainment form [**9**]. This method optimizes the Cholesky factors of the weighting matrices and hence generates only guaranteed stable optimal solutions.

2.3 Control structure

An alternative forward path transfer function form of the PIP control algorithm can be obtained by eliminating the inner loop of Fig. 1a to form the unity feedback control structure shown in Fig. 1b. The feedback and forward path structures of the PIP controller have important consequences, both for the robustness of the final design to parametric uncertainty and for the disturbance rejection characteristics. In particular, while the feedback form is generally more robust to uncertainty in the estimated system dynamics, the unity feedback aspect of the forward path form offers disturbance rejection characteristics that are usually superior, since they are similar in dynamic terms to those associated with the designed command response [**7**]. For this reason, the forward path structure is employed in all the results discussed below.

Another very desirable characteristic of the forward path structure is that, in general, the actuator signal is much smoother than that produced by the feedback form of the controller. For the forward path implementation, the output signal is only filtered through the integral component of the controller, which is a low-pass filter; hence the input variable usually has a relatively low variance even in the presence of measurement noise. This has important practical implications for reducing actuator wear. In the case of the feedback structure the situation is more complex, however, since past noisy values of the disturbed output are involved in the control signal synthesis because of the feedback filters (see reference [**7**] for details).

Note that, whichever PIP structure is chosen, the equivalent *incremental feedback* or *incremental forward path* form of the control algorithm is always used in practice [**6**]. This provides an inherent means of avoiding 'integral wind-up' when the controller is subject to constraints on the actuator signal, as in the present example. Of course, such an *ad hoc* approach does not necessarily yield good control performance and a controller which is specifically designed to handle constraints in an optimal manner would undoubtedly provide superior results, albeit at the cost of a considerably more complex control system design and implementation. The present paper has chosen to look only at designs which are of an implementational complexity similar to conventional two- and three-term controllers.

3 MODEL REDUCTION

The NMSS–PIP approach to control design usually involves identifying transfer function models from meas-

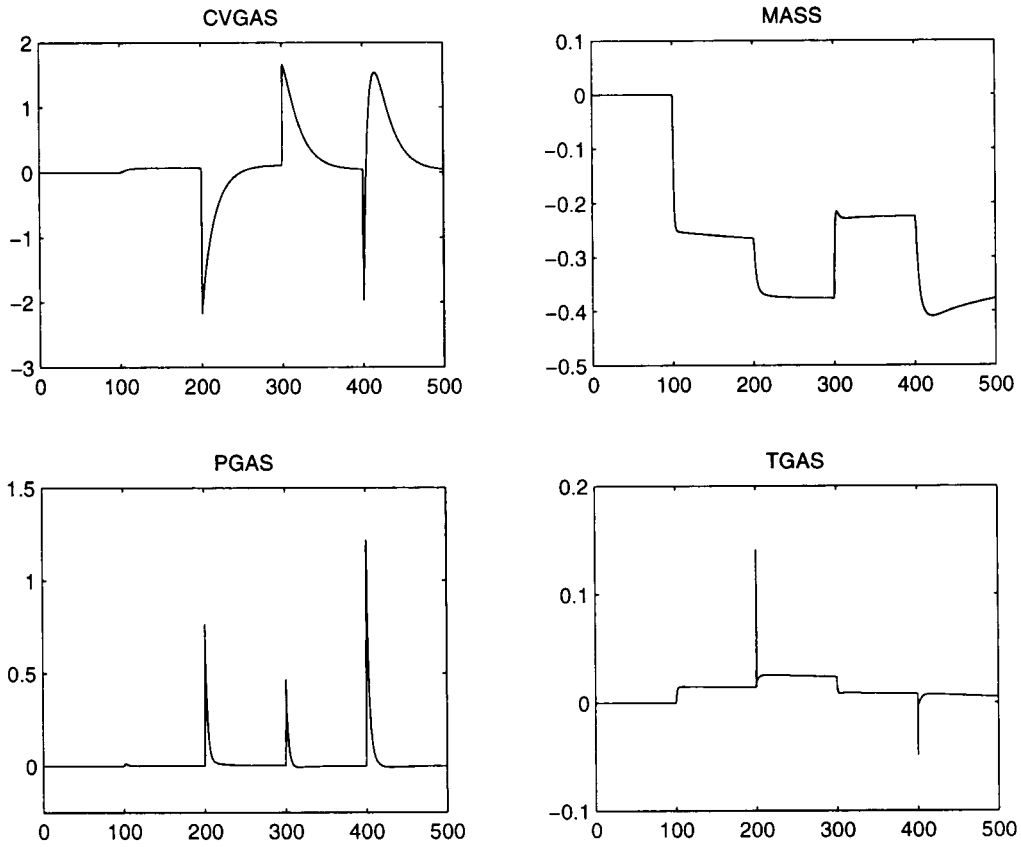

Fig. 2 Open-loop SRIV-estimated reduced-order model response of the gasifier simulation at 100 per cent load to unit impulses in WCHR (kg/s), WAIR (kg/s), WCOL (kg/s) and WSTM (kg/s) at 100, 200, 300 and 400 s. CVGAS (kJ/kg), MASS (kg), PGAS (kN/m^2) and TGAS (K) are plotted against time in seconds; in each case, zero represents the steady state operating point, where the absolute values have been listed by Dixon *et al.* [**8**]. The output of the high-order model is indistinguishable from these reduced-order model responses

ured input–output data collected from the *actual* plant. In this case, an inner loop controller would be employed to maintain the bed mass level at the required set point, so that the other variables behave satisfactorily in the short term. However, since the simulation provided for the benchmark challenge is both linear and stable, this is not a problem in the context of the present *model reduction* exercise. Instead, the main difficulty is that, while the long-term dynamics dominate the open-loop step response, it is the rapid response modes that are of most importance to the specified control objectives. Such modes are best investigated by utilizing simple 'impulse' input signals (or similar short bursts of actuator activity).

The choice of sampling rate is clearly very important for this application. In fact, open-loop experiments indicate that, while the PGAS variable exceeds its allowed limit of 10 kN/m^2 within 2 s of the specified step disturbance, the new steady state conditions are not reached for approximately 24 h. The present research suggests that, while a sampling rate of 0.5 s or faster is required in order to meet the step disturbance control objectives, this means that the slower modes in the system have to be approximated by having some poles very close to the unit circle. Indeed, it may sometimes be useful to approximate these modes with exact integrators (by differencing the simulation data), or by exploitation of singular perturbation methods, although such approaches were not required for the results below. This problem presented by the 'stiff' system is one reason why alternative discrete-time δ operator methods are often useful [**9**].

As will become clear, a conventional z^{-1} operator approach yields a PIP control algorithm that maintains good control of the present benchmark system. Here, a sampling rate of 0.25 s was selected, since this appears to offer an adequate description of the short-term dynamics, while minimizing the aforementioned problems. The reduced-order multiple-input single-output models obtained by SRIV identification and estimation are all third order and their response to impulse inputs is illustrated in Fig. 2. Note that, since the coefficient of determination (R_T^2) values are all in the range 0.994–0.997 (i.e. 99.4–99.7 per cent of the high-order

model response is explained by the third-order models), the outputs are visually indistinguishable from the high-order simulation data, which are also plotted on the graphs.

4 PERFORMANCE TESTS

The performance tests required for the benchmark challenge are based on the response of the control system to the sink pressure disturbance signal PSINK. Two scenarios are considered:

(a) a sine wave disturbance of amplitude 20 kN/m^2 and frequency 0.04 Hz and
(b) a step disturbance of -20 kN/m^2 starting at 30 s.

In each case, the output variables should fluctuate by less than the following limits: CVGAS, 10 kJ/kg; MASS, 500 kg; PGAS, 10 kN/m^2; TGAS, 1 K. Note that these limits, which are plotted as horizontal lines on the graphs that follow, represent the allowed positive or negative variation about the steady state operating point, represented by zero in Figs 3 to 5 later.

4.1 Unconstrained default performance

As an initial evaluation step, the default PIP controller, with the LQ weights $y_1^w, \ldots, y_p^w$, $u_1^w, \ldots, u_p^w$ and $z_1^w, \ldots, z_p^w$ all set to unity, is applied to the gasifier system without any input constraints. As would be expected in this ideal case, the control performance is very good indeed, with the outputs rapidly returning to the set point following the application of the disturbance signal. For example, the maximum errors for the critical CVGAS and PGAS variables are just 0.33 kJ/kg and 3.01 kN/m^2 respectively, well within the required 10 kJ/kg and 10 kN/m^2 design limits. As illustrated by Fig. 3, even at the most difficult 0 per cent load case, the maximum deviations of these two variables, for either disturbance, are 2.66 kJ/kg and 6.12 kN/m^2. However, the main problem with this initial design is that the WCHR and WCOL actuators exceed their specified constraints (for brevity, the input signals are not shown in Fig. 3). In the case of the response to a step disturbance in particular, the peak rate of change of WCOL is 2.23 kg/s^2, over ten times faster than the allowed maximum.

For this unconstrained case, it should be stressed that the four output variables remain well within the specifications for both types of disturbance at *all three operating conditions*. It is clear, therefore, that the PIP algorithm is highly robust to any model uncertainty associated with the various operating points. In this regard, it should be stressed that all the results discussed in the present paper are based on the model reduction exercise for the 100 per cent load case only. Of course, in practice, model mismatch is an important consideration and it would be particularly interesting to apply the PIP design to the full non-linear simulation, which would provide a more challenging and realistic test.

4.2 Performance optimized for robustness

It is clear from the unconstrained simulation experiments that, in the present context, the issue of robustness primarily refers to the ability of the PIP algorithm to handle the input constraints. In this regard, it is straightforward to retune the controller to soften the design requirements and so reduce demands on the actuators. Accordingly, the aim of the following weighting parameters is to penalize the input signals in the LQ cost function, particularly the problematic WCHR and WCOL variables which suffer from highly limiting rate constraints:

$$u_1^w = 100, \qquad u_2^w = 25, \qquad u_3^w = 100, \qquad u_4^w = 25 \tag{12}$$

As before, y_1^w and z_i^w $(i = 1, \ldots, 4)$ are set to the default unity. The retuned PIP algorithm meets all the performance requirements at both the 100 and the 50 per cent load operating points, now with the input constraints fully implemented (Table 1). It is only at the most difficult 0 per cent load operating point that any of the output limits are exceeded, as illustrated by Fig. 4. Note that, because of the incremental form of the controller, the input signals are *never* allowed to violate any of their constraints since this would, in effect, invalidate the benchmark results.

The only practical problem with this PIP LQ design is that the PGAS variable exceeds its 10 kN/m^2 limit at 0 per cent load. In addition, for the sine wave disturbance, the TGAS variable exceeds its limit by 0.43 K during the specified simulation time. This deviation eventually peaks at 1.94 K after about 1000 s. However, note that even 1.94 K is a deviation of less than 0.2 per cent from the absolute value of the set point. Additional tuning yields a reduced PGAS peak level, but at the expense of a poorer response in the other variables. Of course, retuning the controller to obtain optimal performances at the different operating points is not strictly allowed for in the benchmark challenge, where the controller should be derived primarily from the 100 per cent load condition.

4.3 Performance optimized for 100 per cent load

By taking a literal interpretation of the requirement that the controller should be based on the 100 per cent load condition, it is very straightforward to obtain a PIP design that provides improved results at the 100 and 50 per cent load levels. Noting that WCOL is the most problematic input variable, the following weighting parameter is chosen with all the remaining parameters set

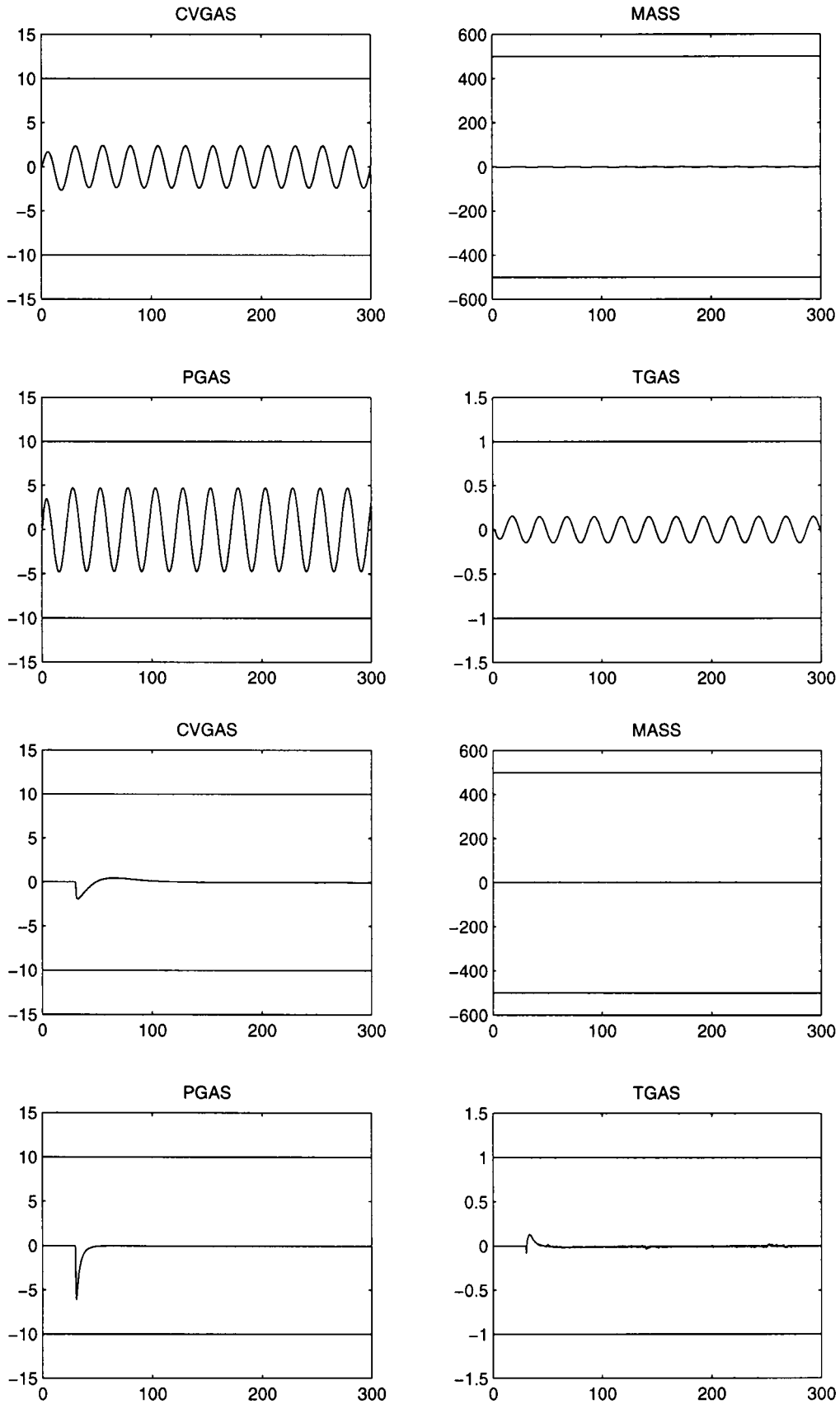

Fig. 3 Default PIP LQ control without input constraints (see Section 4.1); response to sine wave and step disturbances at 0 per cent load (units as in Fig. 2)

Table 1 Performance evaluation table for the PIP controller tuned with $u_1^w = 100$, $u_2^w = 25$, $u_3^w = 100$ and $u_4^w = 25$ (absolute refers to the maximum deviation of the output variable from the set point; maximum and minimum refer to the maximum and (negative) minimum values respectively of the input variable; rate refers to the maximum rate of change of the input variable (kg/s^2); IAE refers to the integral of absolute error; violations of the constraints or output objectives are highlighted in bold; the units employed throughout are equivalent to those listed in the caption of Fig. 2)

Input or output constraint	Step disturbances			Sine wave disturbances		
	100%	50%	0%	100%	50%	0%
CVGAS, absolute	3.04	4.16	7.33	1.14	2.17	6.73
MASS, absolute	0.88	1.31	3.86	0.83	0.84	3.48
PGAS, absolute	6.77	8.36	**12.48**	4.56	6.05	**16.77**
TGAS, absolute	0.41	0.30	0.53	0.12	0.19	**1.43**
WCHR, maximum	0.46	1.23	2.41	0.33	0.25	0.00
WAIR, maximum	1.49	1.96	3.59	1.20	1.45	2.70
WCOL, maximum	1.45	2.54	4.26	0.80	0.91	0.89
WSTM, maximum	1.22	1.54	2.35	0.86	1.20	2.45
WCHR, minimum	0.49	0.47	0.50	0.41	0.34	0.50
WAIR, minimum	0.44	0.65	1.19	1.24	1.48	2.47
WCOL, minimum	0.00	0.00	0.00	0.93	1.09	1.80
WSTM, minimum	0.17	0.41	0.58	0.81	1.15	0.68
WCHR, rate	0.20	0.19	0.20	0.13	0.10	0.20
WAIR, rate	0.73	0.90	1.00	0.50	0.64	1.00
WCOL, rate	0.20	0.20	0.20	0.20	0.20	0.20
WSTM, rate	0.70	0.88	1.00	0.29	0.44	1.00
CVGAS, IAE	189×10^3	34×10^3	73×10^3	201×10^3	366×10^3	836×10^3
PGAS, IAE	239×10^3	55×10^3	108×10^3	839×10^3	1103×10^3	2631×10^3

to the default unity:

$$u_3^w = 100 \tag{13}$$

With these settings, the response to a sine wave disturbance is well within the required specifications for both the 100 per cent (Fig. 5) and 50 per cent load operating points (Table 2). In fact, there is only a relatively small degradation of the performance in the latter case. For example, the variable that comes the closest to its allowed limit is PGAS; at 100 per cent load, the peak absolute value of PGAS is 3.21 kN/m^2 while, at 50 per cent load, it is 4.16 kN/m^2. Both of these are well within the required 10 kN/m^2. As can be seen from Table 2, the other three variables are also maintained very well at both these operating points. Even in the 50 per cent load case, for example, their peak absolute values are as follows: CVGAS, 1.46 kJ/kg; MASS, 0.57 kg; TGAS, 0.39 K. These should be compared with their respective limits of 10 kJ/kg, 500 kg and 1 K.

It is clear from Table 2 that some of the actuators are being utilized to their limit. In particular, both WCHR and WCOL often reach their peak rates of 0.2 kg/s^2. At the 100 and 50 per cent load operating points the system remains stable and well behaved, so that this is not a problem; indeed, it is an indication that the controller is fully utilizing the available power of the input signals to achieve optimum performance. However, at the 0 per cent load operating point, rate or level constraints are activated by all four of the inputs and the overall results are then relatively poor. This is not surprising since the PIP control system was deliberately designed to achieve tight control at the primary 100 per cent load operating point. Of course, by softening the requirements at the design stage, somewhat improved control is possible at 0 per cent load, as discussed in Section 4.2 above.

The response to a step disturbance is similarly within the required specifications for both the 100 and the 50 per cent load operating points (see Table 2). However, as illustrated by Fig. 5, control of the temperature variable (TGAS) appears relatively poor even at the 100 per cent load operating point. This is because the WCOL actuator reaches its maximum input level of 1.45 kg/s only a few samples after the start of the step disturbance. As a result, the remaining actuators take a relatively long time to return the TGAS variable to the exact set-point level. Nevertheless, the resulting deviation of TGAS is less than 1 K, compared with the set point of 1223 K in absolute terms, and such a small offset is unlikely to cause any problems in practice.

It should be stressed that, with this simple design, the offset in TGAS after 300 s is gradually eroded and the performance requirements are never violated. The problem is a consequence of using a linear controller in a non-linear situation (i.e. with input constraints) and it is this aspect of the current design that is stimulating the present authors to apply recently developed non-linear PIP approaches [**16**] to the problem, although this is not discussed in the present paper. Finally, note that, because of the changed *absolute* values of the input and output levels, the aforementioned difficulty does not exist at either the 50 or the 0 per cent load operating points.

5 DISCUSSION OF RESULTS

One major advantage of the PIP formulation is the simplicity of the non-minimal state vector and associated LQ weights. Here, any or all of the input or output signals can be directly penalized in the LQ cost function, which provides for straightforward tuning by practising

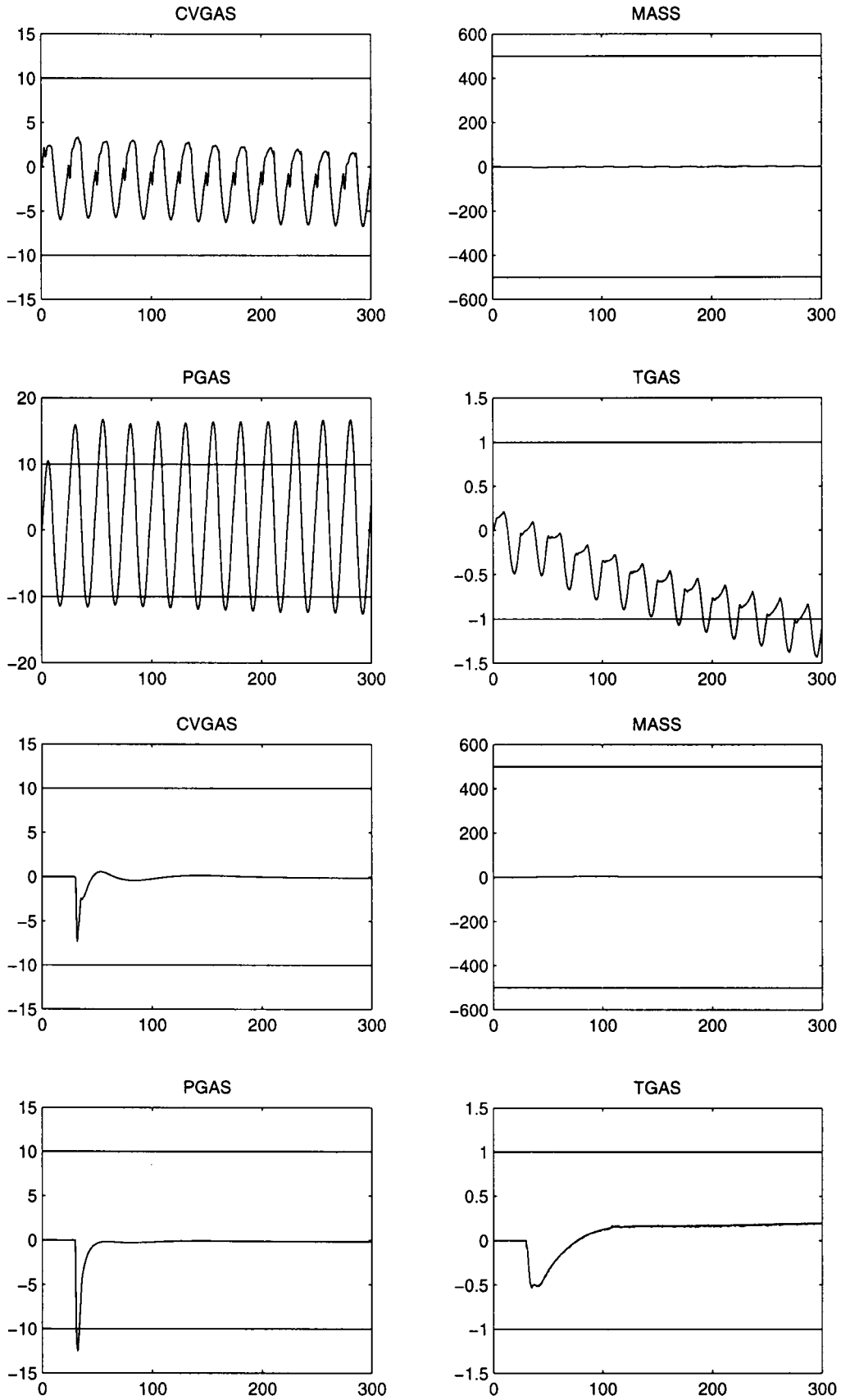

Fig. 4 Response of the PIP LQ control system tuned with $u_1^w = 100$, $u_2^w = 25$, $u_3^w = 100$ and $u_4^w = 25$; sine wave and step disturbances at 0 per cent load (units as in Fig. 2)

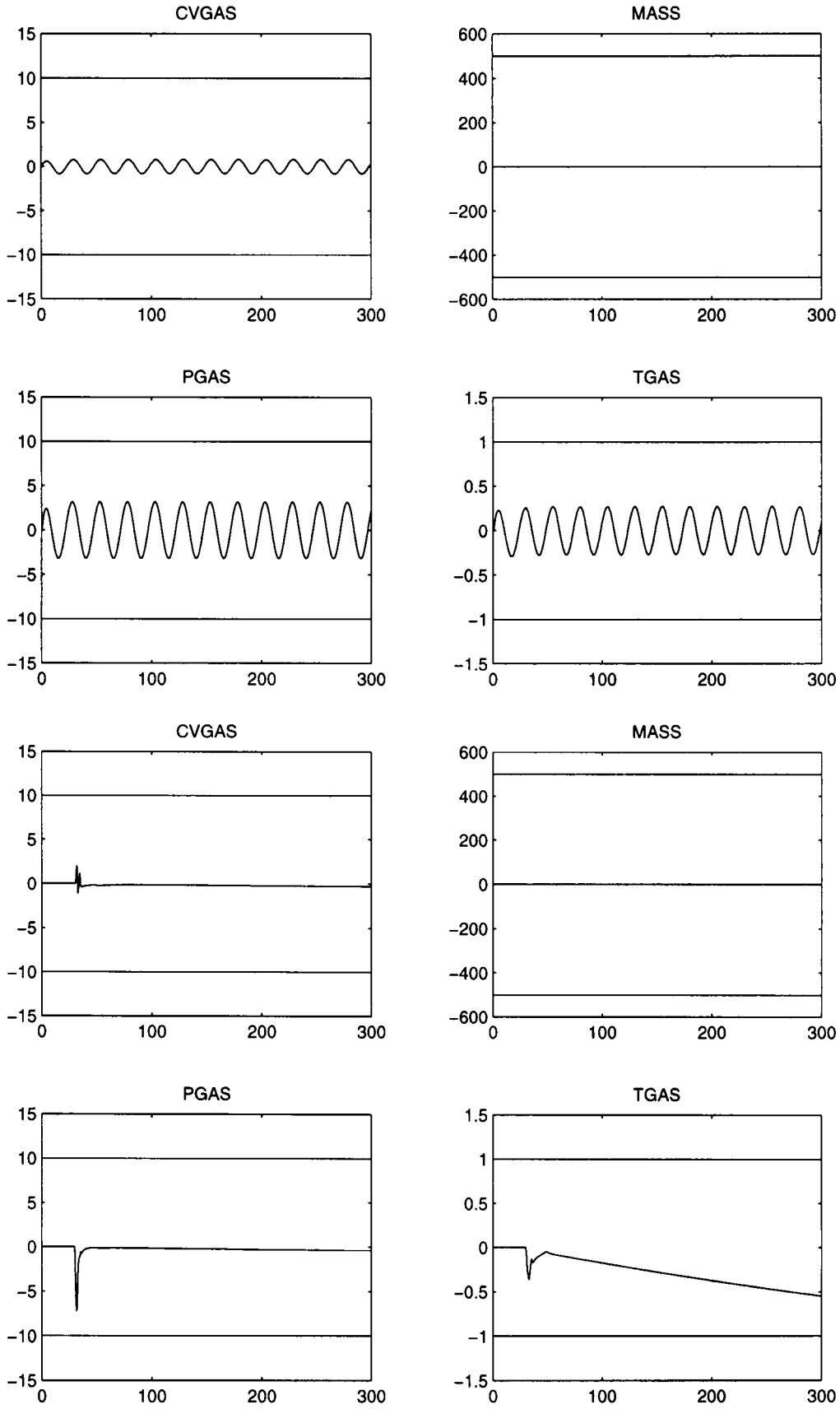

Fig. 5 Response of the PIP LQ control system tuned with $u_3^w = 100$; sine wave and step disturbances at 100 per cent load (units as in Fig. 2)

Table 2 Performance evaluation table for the PIP controller tuned with $u_3^w = 100$ (see the heading of Table 1 for details)

Input or output constraint	Step disturbances			Sine wave disturbances		
	100%	50%	0%	100%	50%	0%
CVGAS, absolute	1.97	3.65	**17.51**	0.86	1.46	**16.53**
MASS, absolute	0.54	0.62	3.55	0.56	0.57	6.68
PGAS, absolute	7.21	9.02	**13.82**	3.21	4.16	**22.80**
TGAS, absolute	0.55	0.46	0.80	0.29	0.39	1.00
WCHR, maximum	0.43	1.13	2.48	0.78	0.74	1.58
WAIR, maximum	1.50	1.93	3.62	1.66	2.08	3.54
WCOL, maximum	1.45	2.42	4.14	0.45	0.52	2.01
WSTM, maximum	2.20	2.51	3.30	1.39	1.82	3.12
WCHR, minimum	0.70	0.53	0.50	0.89	0.89	0.50
WAIR, minimum	1.20	1.30	1.62	1.68	2.10	3.36
WCOL, minimum	0.00	0.00	0.00	0.70	0.80	1.66
WSTM, minimum	0.16	0.35	0.53	1.34	1.69	0.68
WCHR, rate	0.20	0.20	0.20	0.20	0.20	0.20
WAIR, rate	1.00	1.00	1.00	0.72	0.90	1.00
WCOL, rate	0.20	0.20	0.20	0.18	0.20	0.20
WSTM, rate	1.00	1.00	1.00	0.68	0.81	1.00
CVGAS, IAE	59×10^3	21×10^3	128×10^3	151×10^3	259×10^3	1683×10^3
PGAS, IAE	85×10^3	33×10^3	74×10^3	603×10^3	779×10^3	2702×10^3

engineers. This is clearly illustrated by the second PIP design (13), which is based on the simple observation that WCOL exceeds its allowed limit in an unconstrained simulation. By increasing just u_3^w, the resulting controller meets all the design requirements at both the 100 per cent (Fig. 5) and the 50 per cent load operating points (Table 2).

The response to a sine wave disturbance provides a second example of such intuitive tuning. Here, the amplitude of the four output variables can be effectively changed over a wide range by simply adjusting the output weights y_i^w ($i = 1, \ldots, 4$). In Figs 3 to 5 these parameters were set to the default unity; however, should the control objectives demand a reduced amplitude in the ith variable, say, at the expense of the other three outputs, then this is straightforwardly achieved by increasing the y_i^w weighting term.

It should be stressed that, in the present research, the controller has deliberately *not* been optimized for each disturbance and load separately, since this does not make sense from a practical point of view. For example, if good control is required at all three operating points, it would be preferable to estimate a control model and to design the associated controller at the middle 50 per cent load condition, rather than at one of the extremes as in the benchmark challenge. In fact, an even better solution would be to obtain new reduced-order models for each operating point and subsequently to employ a gain scheduled approach, or even a fully adaptive controller, both of which would present only simple design extensions and would provide a good and yet practical design solution in this case [**2**].

The results presented in Table 1, based on the manually retuned PIP algorithm (12), represent one particular judgement by the present authors on what might be most useful overall. In this example, more objective optimization of the LQ weights, as mentioned in Section 2.2 and based on the benchmark objectives, yields very similar results to these. In this multi-objective optimization [**9**], the diagonal and off-diagonal elements of the **Q** and **R** matrices are numerically optimized to meet the specified goals across all three operating points, where these are realizable. In practice, such an approach would benefit from more detailed control objectives, including knowledge of the relative importance of each output variable and whether it is the peak value, or the long-term integral of absolute error, of a given variable that has the most critical effect on the gasifier performance. Although in this case such multi-objective optimization has not proven necessary, in other applications of PIP control, it has been successfully employed to meet design objectives that could *not* be satisfied by straightforward manual tuning (see, for example, reference [**9**]).

6 CONCLUSIONS

This paper has presented the results obtained in a design exercise aimed at producing a multi-variable PIP controller for the ALSTOM gasifier benchmark system that satisfies the closed-loop performance requirements set out in the design challenge description supplied by the company. This discrete-time PIP design, which is based on a backward-shift operator reduced-order model using a single uniform sampling rate, satisfies all the performance requirements at the 100 and 50 per cent load operating points. This has involved a very simple design procedure, with the weights in the LQ cost function used to tune straightforwardly the closed-loop response. However, if other more difficult design objectives are required, the algorithms may be tuned still further by the more computationally intensive multi-objective optimization methods mentioned in Section 5. Whichever approach is employed, the resulting fixed-gain PIP controller is very simple and could be implemented on any computer-controlled system without modifications, other than minor algorithmic changes in the software.

As the next step in the design exercise, it would be interesting to implement the PIP controller on the full non-linear simulation [**8**], which would then provide a more realistic evaluation of the robustness of the designs to model uncertainty. Such simulation experiments would also reveal whether a gain scheduled or adaptive controller [**2**] would be beneficial in practice. Another area of ongoing research is to apply recent developments in identification and control of non-linear systems [**16**] to the problem and this would clearly benefit from the availability of the original simulation. Also, the present authors have recently developed a non-linear PIP algorithm which is able to handle input and output constraints explicitly at the design stage and these findings will be reported in future publications.

It should be stressed that all the results discussed above have assumed that the disturbance is not available for measurement and can only be accounted for in the feedback loop by its effect on the output variables. Although not discussed in the present paper, it is straightforward to introduce additional measured or stochastic input disturbances into the NMSS formulation by simply extending the state vector to include these additional state variables, which can be measured or estimated with a simplified Kalman filter observer [**17**]. The resulting feedforward PIP controller is able to exploit the available measurements to predict and correct for disturbances to the system. Such an approach has been successfully utilized in other PIP applications [**4**].

Finally, it is clear that the main challenge associated with the benchmark system is to prevent violation of the input constraints. By softening these constraints, the default fixed-gain PIP algorithm, without any tuning at all, comfortably meets all the control objectives at each operating point including the most difficult 0 per cent load case (Fig. 3). In practice, therefore, it is clear that changing the actuator devices could provide a relatively straightforward way of greatly improving the control performance. A related engineering solution that could reduce the effect of the disturbance is to provide a reservoir between the gasifier and the turbine, with the objective of maintaining a relatively constant system pressure, in a manner similar to a hydraulic accumulator.

ACKNOWLEDGEMENT

The authors are grateful for the support of the UK Engineering and Physical Sciences Research Council (EPSRC).

REFERENCES

1 **Young, P. C., Behzadi, M. A., Wang, C. L.** and **Chotai, A.** Direct digital and adaptive control by input–output, state variable feedback pole assignment. *Int. J. Control*, 1987, **46**, 1867–1881.

2 **Chotai, A., Young, P. C.** and **Behzadi, M. A.** Self-adaptive design of a non-linear temperature control system. *Proc. Instn Electl Engrs, Part D*, 1991, **38**, 41–49.

3 **Taylor, C. J., Young, P. C.** and **Chotai, A.** On the relationship between GPC and PIP control. In *Advances in Model-Based Predictive Control* (Ed. D. W. Clarke), 1994, pp. 53–68 (Oxford University Press, Oxford).

4 **Young, P. C., Lees, M., Chotai, A., Tych, W.** and **Chalabi, Z. S.** Modelling and PIP control of a glasshouse microclimate. *Control Engng Practice*, 1994, **2**(4), 591–604.

5 **Norris, T. S., Bailey, B. J., Lees, M.** and **Young, P. C.** Design of a controlled ventilation open-top chamber for climate change research. *J. Agric. Engng Res.*, 1996, **64**, 279–288.

6 **Taylor, C. J., Young, P. C., Chotai, A.** and **Whittaker, J.** A non-minimal state space approach to multi-variable ramp metering control of motorway bottlenecks. *Proc. Instn Electl Engrs, Part D*, 1998, **145**(6), 568–574.

7 **Taylor, C. J., Chotai, A.** and **Young, P. C.** Proportional–integral-plus (PIP) control of time delay systems. *Proc. Instn Mech. Engrs, Part I, Journal of Systems and Control Engineering*, 1998, **212**(I1), 37–48.

8 **Dixon, R., Pike, A. W.** and **Donne, M. S.** The ALSTOM benchmark challenge on gasifier control. *Proc. Instn Mech. Engrs, Part I, Journal of Systems and Control Engineering*, 2000, **214**(I6), 389–394.

9 **Chotai, A., Young, P. C., Mckenna, P. G.** and **Tych, W.** Proportional–integral-plus (PIP) design for delta (δ) operator systems. Part 2: MIMO systems. *Int. J. Control*, 1997, **70**, 149–168.

10 **Young, P. C.** Identification, estimation and control of continuous-time and delta operator systems. In *Identification in Engineering Systems* (Eds M. I. Friswell and J. E. Mottershead), 1996, pp. 1–17 (University of Wales, Swansea).

11 **Young, P., Parkinson, S.** and **Lees, M.** Simplicity out of complexity in environmental modelling: Occam's razor revisited. *J. Appl. Statist.*, 1996, **23**, 165–210.

12 **Young P. C.** *Recursive Estimation and Time Series Analysis*, 1984 (Springer-Verlag, Berlin).

13 **Young P. C.** Simplified refined instrumental variable (SRIV) estimation and true digital control (TDC): a tutorial introduction. In Proceedings of the First European Control Conference, Grenoble, France, 1991, pp. 1295–1306.

14 **Chotai, A., Young, P. C.** and **Tych, W.** Dynamic decoupling, pole assignment and servo-mechanism design for multivariable NMSS discrete-time systems. In Proceedings of the Sixth IMA Conference on *Control, Modelling, Computation and Information*, Manchester, 1992.

15 **Borrie, J. A.** *Modern Control Systems: A Manual of Design Methods*, 1986 (Prentice-Hall, Englewood Cliffs, New Jersey).

16 **Young, P. C.** A general approach to identification, estimation and control for a class of nonlinear dynamic systems. In *Identification in Engineering Systems* (Eds M. I. Friswell and J. E. Mottershead), 1996, pp. 436–445 (University of Wales, Swansea).

17 **Hesketh, T.** Linear quadratic methods for adaptive control—a tutorial. Report 765, Control Systems Centre, University of Manchester Institute of Science and Technology, Manchester, 1992.

